Energetics, structures, vibrational frequencies, vibrational absorption, vibrational circular dichroism and Raman intensities of Leu-enkephalin

2003 J. Phys.: Condens. Matter 15 S1823

(http://iopscience.iop.org/0953-8984/15/18/315)

INSTITUTE OF PHYSICS PUBLISHING JOURNAL OF PHYSICS: CONDENSED MATTER

J. Phys.: Condens. Matter **15** (2003) S1823–S1851 PII: S0953-8984(03)55823-4

Energetics, structures, vibrational frequencies, vibrational absorption, vibrational circular dichroism and Raman intensities of Leu-enkephalin

K J Jalkanen

Quantum Protein (QuP) Centre, Department of Physics, Technical University of Denmark, Building 309, DK-2800 Lyngby, Denmark

E-mail: jalkanen@fysik.dtu.dk

Received 8 November 2002, in final form 13 March 2003
Published 28 April 2003
Online at stacks.iop.org/JPhysCM/15/S1823

Abstract

Here we present several low energy conformers of Leu-enkephalin (LeuE) calculated with the density functional theory using the Becke 3LYP hybrid functional and the 6-31G* basis set. The structures, conformational energies, vibrational frequencies, vibrational absorption (VA) intensities, vibrational circular dichroism (VCD) intensities and Raman scattering intensities are reported for the conformers of LeuE which are expected to be populated at room temperature. The species of LeuE present in non-polar solvents is the neutral non-ionic species with the NH_2 and CO_2H groups, in contrast to the zwitterionic neutral species with the NH_3^+ and CO_2^- groups which predominates in aqueous solution and in the crystal. All of our attempts to find the zwitterionic species in the isolated state failed, with the result that a hydrogen atom from the positively charged N-terminus ammonium group transferred either to one of the oxygens of the carboxylate group of the C-terminus or to the oxygen of the amide group of one of the other residues. Hence we conclude that the zwitterionic species of LeuE is not stable in the isolated state. Spectral simulations of the species expected to be found in the isolated state can be compared to the measured VA, VCD and Raman spectra of LeuE in non-polar solvents to identify which conformer or conformers of LeuE are present in these media. Characteristic features in the VCD spectra are more sensitive to conformational changes than those in either the VA or Raman spectra, similar to the characteristic features in electronic circular dichroism spectra with respect to those in the UV–vis electronic absorption spectra. Finally, we have also attempted to stabilize the zwitterionic species by treating the aqueous environment by using a continuum solvent approach, the Onsager model. Here we found that the zwitterionic species is now stable. The neutral species in an aqueous environment was also modelled by the continuum solvent approaches to determine the relative stability of these two species in this new aqueous environment. Here the relative energy of the zwitterionic species is higher than neutral species, in contradiction

to experiment. Hence the use of explicit water molecules plus either this or another continuum model to treat the bulk water environment is necessary to make the zwitterionic species more stable than the neutral species. We are pursuing explicit water molecules to treat LeuE in this environment.

(Some figures in this article are in colour only in the electronic version)

1. Introduction

The recent development of theoretical methods and increased computing power has made it possible to study small peptides and amino acids with *ab initio* quantum mechanical methods [1–9]. Polypeptides, including Leu-enkephalin (LeuE), LALA and N-acetyl L-alanine N′-methyl amide (NALANMA), have predominantly been studied with empirical force fields [5, 10–19] and combined experimental and theoretical methods [1, 6, 8, 20].

Small polypeptides such as LeuE and Met-enkephalin are important molecules from two different perspectives. First, they have more features of proteins than the simpler models for proteins, N-methyl acetamide (NMA) and NALANMA, which have been extensively studied [8, 9, 21]. LeuE has glycine (Gly) residues at positions two and three which give it more flexibility than the other pentapeptides. Here it can form various turn structures, and indeed two of the crystal forms of LeuE are turn structures (a single β bend and a double β bend) [22, 23]. Previously an extended structure for LeuE has also been reported [24, 25]. The structure of Met-enkephalin (MetE) has been found to have a β turn structure in the lyotropic nematic phase [26]. LeuE also has two aromatic residues, L-tyrosine (Tyr) in position one and phenyl-L-alanine (Phy) in position four. Hence the possibility of having π–π interactions from stacked aromatic groups, as found in nucleic acids, is also possible. Here dispersion interactions may be very important. The fifth residue, L-leucine (Leu), is also a hydrophobic residue, so it will affect the structure of the LeuE to the extent that it will not like to be exposed in a hydrophilic environment, but buried in a hydrophobic environment. The relative orientation of the Tyr ring with respect to the peptide backbone and also its accessibility have been shown also to be important for its biological function. Different conformers of LeuE and MetE analogues with different backbone angles (folds), but similar orientations of the Tyr rings, are biologically active [27, 28]. Hence it may not even be the right question to ask what is the backbone fold or conformer of LeuE, MetE and analogues, but what are the required constraints on the spatial orientations of the side chains, which are what seem to interact with the receptor and provide function, and not necessarily the backbone amide groups. Recently, the crystal structure of the LeuE racemate has also been solved [29, 30]. The conformation of the racemate crystal belongs to the extended form. The symmetry-related molecules are connected by hydrogen bonds and arranged in an antiparallel fashion, which results in a sheet structure similar to the natural enkephalin (Enk), that is, with only L-amino acids (L-Tyr–Gly–Gly–L-Phe–L-Leu). A literature review by Deschamps *et al* (1996) reviews structural studies of opioid peptides from 1988 to 1996 [31].

Second, many small polypeptides, such as LeuE and MetE, are biologically active and found endogenously in many animals and humans [32]. Hence the determination of the conformations and spatial orientations of the interacting residues of these biologically active peptides is important. Various conformers of LeuE seem to bind to different receptors and it is usually accompanied by MetE. MetE differs from LeuE in the fifth residue being Met instead of Leu. Hence studying the potential energy surface (PES) of LeuE and other small peptides in

various environments is of interest not only from a purely theoretical point of view, but also to medical researchers who are interested in understanding this molecule (an opiate ligand) and related analogues. For example, the transfer of LeuE from an aqueous hydrophilic phase to the lipid-rich hydrophobic environment of its membrane embedded receptor protein may convert LeuE into a bioactive state (conformer) required for eliciting biological activity. Hence it is very important to also study LeuE in the isolated or hydrophobic environment (in the absence of water molecules). It is also important to synthesize and study agonists and antagonists selective for only one of the opioid receptors. They should also be peptidase resistant and penetrate the blood–brain barrier. This makes it also important to understand the properties of LeuE and its synthetic analogues in both the aqueous and non-polar (hydrophobic) environments.

There have to date been reported several different x-ray structures of biologically active LeuE: an extended structure, a single-β-turn type structure and a double-bend type structure [22–25, 29, 33, 34]. There have also been various theoretically determined structures of LeuE [11–20, 35]. NMR solution data on LeuE have also appeared [36–39], and in addition, NMR structure determinations have been undertaken [26, 27, 36, 40, 41] for biologically active LeuE, MetE, [D-Pen^2, D-Pen^5]-enkephalin (DPDPE) and [D-ala^2]-MetE. Here they have focused on the hydrophobic environment, both in the membrane and in the liquid crystal phase [26–28]. Mutagenesis studies have also been performed to see which residues and conformers are important for biological activity [28].

In the present study we calculate conformers of LeuE using DFT with the Becke 3LYP hybrid potential, starting from different x-ray and model structures of this peptide. The determination of the lowest energy structure of a relatively large molecule such as LeuE (77 atoms) has the substantial complication of having to solve the multiple-minimum problem. Hence, a complete quantum mechanical calculation of the electronic structure and molecular properties for the ground state PES is non-trivial.

Previously, quantum mechanical calculations have mainly been carried out on peptide-like structures of much smaller systems, e.g., NALANMA [6, 8, 9]. The PES of NALANMA *in vacuo* has been studied with Hartree–Fock, Møller–Plesset (MP) perturbation theory and DFT theories [8, 42]. These data provide a reliable basis for benchmarking other more approximate methods. Recently, empirical force fields have been refined and parametrized against a combination of *ab initio* and experimental data and are now able to reproduce the *ab initio* and experimental data not used in the parametrization with very good precision [43–45]. However, in contrast to many empirical force fields, the α helical conformation, α_R, of NALANMA is not a minimum on the PES at the RHF/6-31G*, MP2/6-31G* and Becke 3LYP/6-31G* *ab initio* levels, although it is a very often appearing structural motif in proteins [8, 45]. In addition, the C_7^{eq} conformer of NALANMA is the most stable conformer in NALANMA and small oligomers of L-alanine, whereas it is seldomly found in proteins [8, 9], indicating that despite the high level of theory, application of *ab initio* methods to isolated states of short peptides might provide an inadequate description of the molecular structure of polypeptides and proteins, especially if one is interested in understanding a molecule and its properties in the aqueous environment. Also, the study of and use of small compounds, like NMA and NALANMA, in force field and semi-empirical parametrization, may not be adequate, due to the lack of interactions which stabilize larger peptides and proteins. This motivates our work here on a larger peptide such as LeuE, in addition to its biological significance.

It is known that solvation plays a crucial role for the stability of the different conformations of NALANMA [6]. By applying a quantum chemical reaction field model on the RHF/6-31G* level of theory [42], the α_R conformation of NALANMA is stabilized significantly with respect to the C_7^{eq} conformer of NALANMA. However, the α_R conformer is still not a minimum on the PES. Only by explicitly including water molecules can this conformer be stabilized and become

a minimum on the Becke 3LYP/6-31G* PES [6]. Free energy calculations with empirical force fields also find a significant stabilization of the α_R [43] and other conformers [46] in solution.

In order to overcome the limitations in the application of fully quantum mechanical calculations to large biological systems (system size and linear scalability), and in the application of semi-empirical and empirical methods (insufficient approximations made in the potential energy functionals and the parametrization thereof), new semi-empirical methods have recently been developed [47, 48]. Results obtained using the SCC-DFTB method have been reported for a variety of small (bio)molecules [49–53]. Along these lines, Lee and Zimmerman recently compared ϕ–ψ potential energy maps, the so called Ramachandran plots, for the isolated state of NALANMA using the AMBER, AMBER3, BIO85, CFF91, CVFF, MM2, MM3, MM+ and SYBYL molecular mechanics (MM) force fields [54]. The more standard semi-empirical methods, the AM1 and PM3 methods, continue to be used however, as the newer methods remain to gain widespread use, due to the limited availability of publicly available codes.

Most of the previous work on documenting methodology using high level quantum calculations has been performed on relatively small bio-molecules. It is also interesting to investigate how the standard semi-empirical methods, e.g., AM1 and PM3, perform against high level Becke 3LYP and MP2 level calculations. Our calculations here provide a good test set for MM force fields and semi-empirical methods which are intended for use on modelling biological systems, in particular peptides and proteins.

In this work, we calculate the relative conformational energies of selected low energy structures of LeuE starting from either x-ray determined structures of all non-hydrogen atoms [22–25] or from six different model structures of LeuE. To each of the crystal structures were added hydrogen atoms. This resulted in 30 different starting structures in total, including the six model structures. All structures were optimized at the SCC-DFTB level with and without a dispersion correction [52], at the B3LYP/6-31G*, AM1, PM3 and MM levels [55]. The six model conformations of LeuE are based on the so called C_7^{eq}, C_7^{ax}, C_5^{ext} (linear) and α_R structures from NALANMA. In this work only the Becke 3LYP/6-31G* results are discussed as they are thought to be the most accurate and do not involve any empirical corrections. Additionally, a structure optimized to the neutral non-ionic form of LeuE even though we started with the neutral zwitterionic form with the positively charged ammonium and negatively charged carboxylate groups. The proton transferred from the ammonium group of the N-terminus residue to the closest oxygen of the carboylate group of the C-terminus residue during the course of the geometry optimization.

In the present work, we study the neutral non-ionic species of isolated state LeuE. In non-polar solvents, which resembles most closely the isolated state, the structure of LeuE is the neutral non-ionic species, that is, with the neutral $-NH_2$ and $-CO_2H$ groups, rather than the neutral zwitterionic species with the charged NH_3^+ and CO_2^- groups as found in aqueous solution at neutral pH and in solid state crystals [34]. In these environments the neutral zwitterionic species is stabilized by either peptide–solvent (water) interactions that are not present in non-polar solvents or by intermolecular interactions between adjacent molecules in the unit cell (crystal environment). Hence taking into account the environment of LeuE is very important in both experimental as well as theoretical studies of this molecule, and most likely the environment profoundly affects the biological function of LeuE [23–25, 38, 56].

In the next section, we give a short description of the methodology used in our structure optimizations and subsequent vibrational frequency, VA, VCD and Raman intensity calculations. Thereafter, we discuss optimization results obtained at the Becke 3LYP/6-31G* level. From these results we propose which structures of LeuE should be populated at room temperature in non-polar solvents. Finally, we present the simulated VA, VCD and Raman

spectra for the low energy conformers of LeuE, with the hope that these simulations will motivate the measurement of the VA, VCD and Raman of LeuE in non-polar solvents and in the membrane (lipid) environment, where LeuE is thought to be functional, since the receptor to which it binds is membrane bound and not floating freely in the cytoplasm. In aqueous solution there appears to be a mixture of the three different conformers of LeuE for which there exist crystal structures. Here we have attempted to determine the change in those structures which occur when the peptide comes into a hydrophobic environment (here modelled by being in the isolated state).

2. Methods

In the following we give a brief description of the methods used to calculate structures and relative energies of LeuE.

*2.1. Becke 3LYP/6-31G**

The Becke 3LYP/6-31G* method is a hybrid DFT method where the exchange–correlation (XC) functional is defined by

$$E^{XC}_{Becke\,3LYP} = E^{X}_{LDA} + c_o(E^{X}_{HF} - E^{X}_{LDA}) + c_X \Delta E^{X}_{B88} + E^{C}_{VWN3} + c_C(E^{C}_{LYP} - E^{C}_{VWN3}) \quad (1)$$

where $c_o = 0.20$, $c_X = 0.72$ and $c_C = 0.81$ [57]. These parameter values were specified by Becke by fitting to atomization energies, ionization potentials, proton affinities and first-row atomic energies in the G1 molecule set [58–63]. Recently, Jalkanen and Suhai have shown that the Becke 3LYP/6-31G* method accurately reproduces gas phase and non-polar solution geometries, vibrational frequencies, and VA and VCD intensities [8]. This level of theory has been documented to model structures and VA spectra of NALANMA, LA and LALA in aqueous solution by adding explicit waters to take into account the first solvation shell which strongly interacts with the peptide as well as the Onsager continuum model added to take into account the interaction of the peptide with bulk water [1, 5–7]. At this level of theory, we are confident that many properties of interest for small peptides, i.e., structural parameters, vibrational frequencies, and relative VA intensities, can be accurately modelled.

2.2. Structure building for non-ionic neutral species

Model structures for the optimization were created using the coordinates of the heavy atoms from the available x-ray data. In general, there are different non-equivalent molecules in the crystallographic unit cell. This resulted in two models for the so called extended LeuE structure of Griffin (labelled e1 and e2), four models for the LeuE extended structure of Karle (labelled e3–e6), four models for the so called single-bend LeuE structure of Smith (labelled s1–s4) and, finally, one model for the so called double-bend LeuE structure of Aubry (labelled d1). Hydrogen atoms were added to the x-ray structures with the program Babel [64], using standard bond lengths and angles [55].

Special attention was paid to the location of the hydrogens in the terminal carboxyl and amine groups, since these may participate in intramolecular hydrogen bonding. A first set of trial structures was generated with the carboxyl group in anti-conformation and the two H–N–C alpha-C dihedral angles set to 180° and −60°, respectively. This choice does not lead to a close contact of possible donors and acceptors and prevents biasing the conformational search towards H-bonded structures. However, from the single-bend conformers only the s4 conformer did not relax to a hydrogen-bonded structure involving the N-terminus. We therefore added one trial structure (s5) equivalent to s4 but with one of the amine hydrogens

directed towards the possible acceptor, the backbone amide oxygen of the Phe residue (PheO). While the orientation of the amine group can be expected to be of major importance only for the single-bend conformers, a hydrogen bond between the carboxyl hydrogen and PheO should be possible for all structural motifs. Because of this we added the trial structures e7–e12 for the extended motif, s6–s10 for the single bend and d2 for the double bend. Here the carboxyl hydrogen was brought into closest contact with PheO while maintaining the O–H bond length and the C–O–H angle in order to facilitate hydrogen bonding. Additionally, we checked for the s4 conformer whether rotation of the amine group in 30° steps as well as whether positioning of the carboxyl hydrogen on the two oxygens in *syn* and *anti* conformation, respectively, resulted in new minima. This was not the case. Certainly, the approach presented here is by no means a stringent conformational search. However, we only focus on finding general differences in the structural and energetical relations between the principal motifs as we have done for NALANMA [8]. In addition to the structures generated from crystal structures, we have also set the backbone angles of the two Gly residues to those found to be of low energy in NALANMA, the alanine dipeptide. Here the C_7^{eq} and C_7^{ax} conformers are degenerate. The C_5^{ext} (extended or linear) structure is also added, as well as the α_R (3.6_{13}) helical structure. Hence we have added the low energy structures predicted from the simple NALANMA model for proteins.

2.3. Geometry optimizations

2.3.1. Neutral non-ionic species. Initially, three hydrogens were added (by Babel [64]) to the N-terminus and no hydrogens were added to the C-terminus, which is consistent with the neutral zwitterionic structure. Subsequent geometry optimizations starting with these structures resulted in the proton from the ammonium group (NH_3^+) being transferred to an adjacent group, i.e., the zwitterionic structure was not stable. This is consistent with our previous works on L-alanine [3, 4, 7, 65] and L-alanyl-L-alanine [1, 5]. Hence, the species for which we have carried out optimizations is the neutral non-ionic species.

The Becke 3LYP/6-31G* geometry optimizations were all performed with the default optimizer in Gaussian 98 [57]. Hessians were calculated for all optimized geometries. The Hessians were used to test whether the optimized structures were indeed local minima, or possibly transition states. The starting point for all of the Becke 3LYP/6-31G* geometry optimizations was the SCC-DFTB (without the dispersion correction (ndp) and with the dispersion correction (dp) [SCC-DFTB-D] optimized structures [55].

In addition to the neutral non-ionic species of LeuE which we determined by adding the two hydrogens to the N-terminus nitrogen and one to one of the carboxylate group oxygens of the C-terminus, we found another neutral non-ionic species by starting the geometry optimization from the neutral zwitterionic species, labelled the s10zwit structure in table 1. Note that this structure is 6.54 kcal mol^{-1} higher in energy than the s10ndp structure, which started from the SCC-DFTB optimized structure.

In addition to modelling the neutral non-ionic species of LeuE in the isolated state, we have modelled this species with the Onsager continuum model [66].

2.3.2. Neutral zwitterionic species. In addition to determining the Becke 3LYP/6-31G* structures of the neutral non-ionic species of LeuE, we have also attempted to determine the structure of the neutral zwitterionic species. Starting from the crystal structure one has the choice of orientation for the hydrogens which we add to the nitrogen of the N-terminus and also to which oxygen of the carboxylate group of the C-terminus and then also which orientation for the hydrogen which we add to the oxygen, this being for the neutral non-ionic species.

Table 1. Relative energies of the different conformers of LeuE for different methods as described in the text. DFT-GGA refers to the hybrid method Becke 3LYP of Becke and Lee, Yang and Parr.

Conf.	Becke 3LYP/6-31G*	ϕ_1'	ϕ_1''	ψ_1	ξ_1	ξ_2	τ_{CCOH}	ϕ_2	ψ_2	ϕ_3	ψ_3	ϕ_4	ψ_4	ξ_1	ξ_2	ϕ_5	ψ_5'	τ_{CCOH}	ξ_1	ξ_2'	ξ_2''
s10ndp	−1889.687 133(0.00)	77	−169	97	−56	92	1	67	12	112	−23	−80	80	−66	98	−79	61	−2	−62	−56	180
s10dp	−1889.682 375(2.98)	80	−167	91	−56	91	1	67	8	111	−24	−79	85	−63	99	−75	118	7	−65	−60	177
s10zwit	−1889.676 706(6.54)	−48	−166	137	−63	91	−1	79	8	109	−24	−82	174	−59	97	−44	−35	150	−61	−59	177
s4ndp	−1889.686 769(0.22)	80	−165	82	−62	91	0	67	6	110	−24	−68	138	−68	99	−133	160	177	−61	−65	172
s4dp	−1889.679 817(4.58)	84	−160	11	−62	85	0	76	12	111	−25	−78	169	−64	96	−71	162	−176	−60	−61	175
s5ndp/dp	−1889.686 769(0.22)	80	−165	82	−62	91	0	67	6	109	−24	−68	138	−68	99	−133	160	177	−61	−65	172
s7ndp	−1889.685 539(0.99)	81	−164	28	−52	116	2	70	24	114	−25	−82	78	−68	98	−78	60	−3	−63	−60	177
s7dp	−1889.681 702(3.40)	−81	163	66	−67	93	1	66	22	109	−23	−80	86	−70	96	−111	6	−2	−76	−63	174
s8ndp	−1889.680 702(4.03)	50	−66	165	−76	65	0	71	25	113	−29	−82	81	−67	97	−78	61	−2	−64	−60	177
s8dp	−1889.674 978(7.63)	49	−67	165	−76	66	0	70	25	114	−31	−81	83	−67	97	128	17	−3	−66	−63	173
s9ndp	−1889.685 539(0.99)	81	−165	29	−52	115	2	71	23	114	−26	−82	78	−68	98	−78	61	−3	−63	−60	177
s9dp	−1889.677 550(6.00)	74	−171	40	−60	104	1	76	20	122	−39	−67	146	−63	100	−115	13	−5	−63	−62	175
eqeqndp	−1889.679 312(4.91)	41	−73	146	−73	72	0	−80	62	−81	61	−84	75	−162	85	−78	61	−3	−63	−60	177
eqeqdp	−1889.679 312(4.91)																				
axaxndp	−1889.679 308(4.91)	47	−66	148	−172	75	1	83	−60	81	−64	−80	76	−163	85	−80	65	−6	−146	−59	177
axaxdp	−1889.678 909(5.16)	48	−66	147	−173	74	2	82	−47	82	−72	−80	74	−164	85	−82	63	−4	−143	−60	176
axeqndp	−1889.679 139(5.02)	42	−72	148	−73	71	0	81	−67	−79	66	−84	73	−161	85	−78	61	−3	−63	−60	177
axeqdp	−1889.679 168(5.00)	42	−73	147	−73	72	0	81	−65	−79	67	−84	74	−162	83	−78	61	−3	−63	−60	177
eqaxndp	−1889.672 740(9.03)	52	−60	166	−165	61	1	−80	58	80	−64	74	−63	−157	164	−76	67	−6	−147	−58	177
eqaxdp	−1889.675 170(7.51)	53	−60	163	−166	57	2	−80	57	79	−68	73	−62	−173	76	−76	67	−6	−146	−59	177

Table 1. (Continued.)

Conf.	Becke 3LYP/6-31G*	ϕ_1'	ϕ_1''	ψ_1	ξ_1	ξ_2	τ_{CCOH}	ϕ_2	ψ_2	ϕ_3	ψ_3	ϕ_4	ψ_4	ξ_1	ξ_2	ϕ_5	ψ_5'	τ_{CCOH}	ξ_1	ξ_2'	ξ_2''
linearndp	−1889.677 610(5.98)	37	−76	152	−71	74	0	−179	179	176	180	−159	178	−149	69	−109	170	179	−59	−60	176
lineardp	−1889.677 608(5.98)																				
s2ndp	−1889.677 204(6.22)																				
s2dp	−1889.673 456(8.58)	93	−170	113	−51	92	3	73	18	121	−33	−71	179	−60	100	−104	146	−176	−59	−59	177
s3ndp	−1889.677 204(6.22)																				
s3dp	−1889.677 204(6.22)	−178	−59	144	−62	92	0	67	21	121	−35	−67	137	−67	101	−134	161	177	−61	−64	172
e5ndp	−1889.669 036(11.35)	47	−65	167	61	95	−179	173	177	179	180	−129	153	−61	96	−145	−35	−178	−179	57	−179
e5dp	−1889.669 658(11.15)	53	−58	175	65	97	180	−138	179	169	−177	−130	153	−59	98	−144	−36	−178	−178	58	−178
s1ndp	−1889.675 844(7.09)	−178	−59	160	−61	91	0	70	24	117	−31	−79	88	−66	102	−112	3	179	−58	−58	178
s1dp	−1889.675 261(7.46)	−178	−59	148	−62	92	0	68	22	119	−33	−70	129	−68	101	−125	−28	−177	−60	−62	175
d2ndp	−1889.676 440(6.70)	57	174	118	−179	70	178	−71	−16	−60	−23	−67	−6	−70	109	−100	3	1	−173	55	178
d2dp	−1889.676 440(6.70)																				
d1ndp	−1889.675 531(7.27)	56	−158	119	−179	68	178	−67	−23	−74	1	−110	12	−61	157	−62	144	178	−175	61	−176
d1dp	−1889.675 530(7.27)																				
e4ndp	−1889.673 646(8.45)	57	−55	178	64	96	0	−143	−175	−172	179	−130	153	−59	97	−138	144	122	−63	−65	171
e4dp	−1889.673 646(8.46)																				
e1ndp	−1889.676 052(6.94)	47	−66	128	−177	86	0	−174	−177	180	−179	−159	156	−169	70	−156	156	177	−175	58	−178
e1dp	−1889.676 051(6.95)																				
s6ndp	−1889.678 607(5.36)	−177	−58	165	−62	92	0	70	23	114	−29	−80	82	−66	102	−79	61	−2	−63	−59	178
s6dp	−1889.674 978(7.63)	49	−67	88	−76	66	0	71	25	114	−31	−81	83	−67	97	−128	17	−3	−67	−63	173
e2ndp	−1889.670 790(10.25)	49	−62	167	61	93	−1	167	−179	−174	−179	−129	154	−60	97	−156	171	178	76	−60	176

Table 1. (Continued.)

Conf.	Becke 3LYP/6-31G*	ϕ_1'	ϕ_1''	ψ_1	ξ_1	ξ_2	τ_{CCOH}	ϕ_2	ψ_2	ϕ_3	ψ_3	ϕ_4	ψ_4	ξ_1	ξ_2	ϕ_5	ψ_5'	τ_{CCOH}	ξ_1	ξ_2'	ξ_2''
e2dp	−1889.667 776(12.15)	37	156	159	67	96	−1	−133	−175	−167	176	−131	155	−59	98	−155	171	178	76	−60	176
e6ndp/dp	−1889.674 665(7.82)	48	−65	126	−176	88	0	−178	−177	−178	180	−130	153	−60	97	−129	166	178	−63	−65	171
e9ndp	−1889.670 015(10.73)	50	166	123	−178	86	0	179	−178	179	−178	−122	141	−62	95	−77	62	−2	−62	−62	174
e9dp	−1889.663 387(14.90)	50	167	121	−178	88	0	177	180	−178	179	−127	150	−59	97	−124	19	−2	−63	−62	175
e3ndp	−1889.674 633(7.84)	48	−65	126	−176	88	0	−179	−176	−175	178	−131	155	−61	97	−123	166	178	−61	−62	174
e3dp	−1889.674 665(7.82)	48	−65	126	−176	88	0	−178	−177	−178	180	−130	153	−60	97	−129	166	178	−63	−65	171
e7ndp	−1889.676 814(6.48)	48	−66	128	−177	86	0	−177	−179	172	178	−159	155	−174	76	−75	66	−3	−169	65	−171
e7dp	−1889.673 078(8.82)	46	−67	135	174	73	−17	−153	171	114	−136	−150	−172	−151	66	−143	158	−3	−174	61	−176
e10ndp/dp	−1889.666 607(12.87)	41	158	151	56	86	−2	171	174	170	−178	−124	140	−60	100	−77	62	−2	−62	−61	175
e11ndp/dp	−1889.663 294(14.96)	47	−64	167	62	95	−179	174	178	−179	180	−130	154	−60	96	−155	161	−3	−176	60	−177
aRndp	−1889.663 663(14.73)	65	−64	1	−69	88	0	−65	−30	−64	−15	−102	−51	−179	34	−137	32	−2	−67	−64	173
aRdp	−1889.666 690(12.83)	65	−64	16	−70	83	−1	61	−125	−71	−1	−86	−88	176	51	−135	71	−13	−65	−65	171
e12ndp/dp	−1889.663 386(14.89)	51	167	121	−178	88	0	177	180	180	179	−126	150	−59	97	−125	19	−2	−63	−62	175
e8ndp	−1889.661 934(15.80)	50	−62	167	61	93	−1	166	−179	−174	−179	−129	154	−60	97	−156	173	−1	77	−59	177
e8dp	−1889.658 901(17.72)	37	156	159	66	96	−1	−132	−175	−167	176	−131	155	−60	98	−156	173	−1	77	−60	176
New	−1889.650 071(23.26)	−154	−34	−161	−167	61	178	−70	−39	−113	−17	−134	62	−59	102	21	−11	169	179	58	−179

However, for the neutral zwitterionic species the N-terminus nitrogen receives three hydrogens, then there is no real choice or ambiguity here. Also, since one does not now need to add an additional hydrogen to either of the two C-terminus oxygens, there is again no choice or ambiguity. Hence this part of the structure determination problem is initially easier. But the problem now is how to treat the aqueous environment. Since the neutral non-ionic species is stable without treating the environment, it is also possible to ignore the environment in the zeroth order treatment of that species. Starting from the same crystal structure which we utilized for the s10 neutral non-ionic species, we have added an additional hydrogen to the N-terminus nitrogen and deleted the hydrogen from the C-terminus oxygen. Our initial attempt to find a stable neutral zwitterionic structure failed however. There was found no barrier to proton transfer from the N-terminus nitrogen to the closest oxygen of the C-terminus, when the carboxylate was indeed closer to the N-terminus hydrogens than the other residue oxygens of their backbone amide groups. In the case where the oxygen of the amide groups of the Phe residue was closer to the hydrogens of the N-terminus nitrogen, there was found no barrier to the transfer of the closest hydrogen to the oxygen of the Phe residue amide group oxygen accompanied by a concerted bond formation between the C′ carbon and the closest oxygen of the C-terminus carboxylate group to form a five-membered ring. This occurred starting from the double-bend crystal structure d2. The backbone angles of this structure are also reported for this chemically modified LeuE, labelled 'New' in table 1. Due to our two failed attempts to find the neutral zwitterionic species without treating the aqueous environment, it was decided to initially treat the aqueous environment with a continuum model approach. There are many different continuum models, and it was decided to choose one of the simplest, the Onsager model, and one of the more recent extensions, the COSMO model. We used as an initial structure the same structure which was generated from the s10 crystal structure, which failed to be a minimum in the absence of any treatment of the environment, and converted to the chemically modifed LeuE. We were able to get a stable neutral zwitterionic structure at the Onsager level of theory.

2.4. Vibrational frequencies, VA, VCD and Raman intensities

In addition to utilizing the Hessians to determine whether the optimized structures are local minima or transition states, the Hessians can also be used to determine the harmonic frequencies and also the eigenvectors (atomic motions during the vibrations). To evaluate the VA intensities one requires the atomic polar tensors (APTs), that is, the derivatives of the electric dipole moment with respect to displacement of the atomic nuclei [67, 68]. To evaluate the VCD intensities, one requires, in addition to the Hessians and APTs, the atomic axial tensors (AATs). Here one requires the momentum derivative of the magnetic dipole moment [69–73]. To date the AAT tensors have been implemented by a variety of formalisms, at the self-consistent field (SCF), multiconfiguration SCF (MCSCF) and DFT levels of theory [73–80]. To evaluate the Raman scattering intensities, one requires in addition to the Hessian the electric dipole–electric dipole polarizability derivatives (EDEDPDs). These tensor derivatives have been implemented at the restricted Hartree–Fock level [81, 82] and recently also at the DFT level [83].

In this work here the APT, AAT and EDEDPD are all calculated at the same level of theory as the geometry optimizations and Hessians, that is, at the Becke 3LYP/6-31G* level. This level of theory has been shown to give very good comparisons to the measured VA and VCD spectra for NALANMA in non-polar and polar solvents [6, 8], the Raman spectra for 3-methylindole in non-polar solvents [84] and the Raman spectra of NALANMA in polar solvents [6]. Hence we feel confident that our VA, VCD and Raman intensities are accurate and reliable and can be used to check whether indeed the predicted low energy conformers predicted are actually present in the given non-polar solvents.

3. Results and discussion

In this section we discuss the results of our theoretical treatment of the low energy conformers present of LeuE in both the neutral non-ionic and zwitterionic forms in both non-polar solvents and in the isolated state. In addition we have attempted to determine both species in aqueous solution, here initially only by use of the continuum solvent models. In a future work we shall also present our work using explicit water molecules and finally explicit water molecules combined with a continuum solvent treatment. Here the continuum model is used to treat the effects due to bulk water. Initially we wanted to see whether, by using only a continuum solvent treatment, we would be able to stabilize the neutral zwitterionic form. This is similar to our previous works on both LA and LALA where a continuum model has been used to treat the effects due to the aqueous solvent [1, 3–5, 65, 85]. Since the treatment of the first solvation shell water molecules via explicit waters and the bulk waters via a continuum solvent model is much more involved, we leave it for a future publication.

3.1. Energetics

In table 1 we present the relative energies for the structures for which we have performed geometry optimizations starting from the SCC-DFTB (ndb) and SCC-DFTB-D (dp) optimized geometries with the DFT method with the Becke 3LYP hybrid exchange correlation potential and the 6-31G* basis set [55]. Many of the low energy structures are those found in crystallographic studies, e.g., the single-β-bend structure, the extended form found in anti-parallel β-sheets and the double-β-bend structure. The six additional model structures have the backbone ϕ and ψ angles found for the three lowest energy conformers found in NALANMA and N-acetyl glycine N′-methylamide, that is, the C_7^{eq} (eq), C_5^{ext} (lin) and C_7^{ax} (ax) conformers. In addition, the α_R or α helix (3.6_{13} helix) is also a very commonly observed motif in peptides and proteins. Hence it is interesting to see whether this structure is stable and also what the relative energy of this structure is with respect to the lowest energy structure. The backbone and side chain torsion angles are all given to completely identify the conformers in table 1, with the knowledge that all of the peptide bonds are in the *trans* conformation. The linear structure of LeuE is presented in figure 1.

In table 1 the relative energies of the conformers determined at the Becke 3LYP/6-31G* level of theory are presented. Here we find only two structures which are within 2.0 kcal mol^{-1} of the lowest energy s10ndp [0.00] structure (LES), the s4ndp and the s7ndp structures, which are 0.22 and 0.99 kcal mol^{-1} higher in energy, respectively. The s5ndp is 2.37 kcal mol^{-1} higher in energy than the LES. As one can see in table 1, the two lowest energy conformers, s10ndp and s4ndp, differ in the orientation of the Tyr residue as exemplified by χ_2 and τ_{COOH}, ψ_2, ψ_4, ϕ_5, ϕ'_5 and τ_{CCOH}. The other backbone and side chain torsion angles are the same. The s10ndp structure is stabilized by a hydrogen bond between the oxygen of the carbonyl C=O amide group of the Tyr residue (1) and the hydrogen of the NH amide group of the Phe residue (4). Here we get a 3_{10} turnlike structure. In addition there is a C_7^{eq} type hydrogen bond between the oxygen of the carbonyl C=O amide group of Gly residue (3) with the hydrogen of the Leu residue (5). Finally, the oxygen of the carbonyl C=O amide group of the Phe residue (4) forms a bifurcated hydrogen bond with both a hydrogen of the amine group of the N-terminus residue (1) and the hydrogen of the OH group on the carboxylic acid C-terminus residue (5). These four stabilizing hydrogen bonds make this conformer the lowest energy structure for LeuE. The s4ndp structure differs by not having two of the hydrogen bonds in conformer s10ndp, but having an additional hydrogen bond between the nitrogen lone pair of the amine group of the N-terminus residue (1) and the hydrogen of the NH amide group of the Gly residue (3).

There exists a hydrogen bond between the oxygen of the carbonyl amide group of the Phe residue (4) and the hydrogen of the NH amine group of the N-terminus residue (1), but no hydrogen bond between this oxygen and the hydrogen of the OH group of the carboxylic acid C-terminus residue (5) due to hydrogen being in the *trans* orientation rather then the *cis* orientation required for hydrogen bonding. The s10dp optimized structure is 2.98 kcal mol^{-1} higher in energy than the s10ndp optimized structure, and differs in only the orientation of the last residue, with the ϕ'_5 angle being such that now the hydrogen bond is between the hydrogen of the OH group of the carboxylic acid C-terminus residue (5) and the nitrogen of the amide group of the same residue (5), forming a five-membered ring instead of the seven-membered ring. This accounts for the higher energy of this structure. With no hydrogen bonding possible with other species in the isolated state or dissolved in a non-hydrogen-bonding solvent, these intermolecularly hydrogen-bonded conformers are the lowest energy structures.

The difference in energy between the eqaxndp and eqaxdp structures is only due to the χ_2 angle of the Phe residue being rotated by approximately 90°. There is an extra 1.5 kcal mol^{-1} stabilization due to π–π interaction between the two aromatic rings, but both structures are local minima. The modes at 38 and 54 cm^{-1} in the eqaxdp structure are the modes where the two aromatic rings rotate in phase with each respect to each other and about their respective C_β–C_γ bonds.

The d2ndp structure has three 3_{10} hydrogen bonds, between residues 1 and 3, 2 and 4, and 3 and 5, with the last hydrogen bond being with the hydrogen of the OH group instead of the hydrogen of the NH amide group of the last residue which is clearly absent in a pentapeptide. This structure is 6.7 kcal mol^{-1} higher in energy than the s10ndp structure, so even though the 3_{10} structure appears to be a stable conformer in LeuE in non-polar solvents, it is not the global minimum. But here there is no interaction and/or stabilizing interaction between the bulky hydrophobic side chains. In a membrane or non-polar solvent, there may be a stabilizing interaction which makes either the 3.6_{13} or 3_{10} structure the lowest energy conformer for this sequence in that environment. As both the 3.6_{13} or 3_{10} helical structures are found in proteins, but the structures do not seem to be the global minima even for those sequences for which they are stable local minima, then it is probably these side chain interactions which make this structure the lowest energy stable structure for this sequence. Hence we need to take into account the environment of the side chains and the stabilizing interactions which make the local structures the global minima, in addition to the hydrogen bonding properties of the backbone amide groups, the charged N-terminus and the C-terminus groups. The d1ndp structure has two of the three 3_{10} hydrogen bonds of the d2ndp structure, the last hydrogen bond being missing due to the hydrogen being attached (bonded) to the other oxygen of the carboxylic group of the C-terminus residue. Also, the relative orientation of the two aromatic groups is different, in this case perpendicular to each other. Hence even though there is a hydrogen bond missing, the energy difference is only 0.5 kcal mol^{-1}.

From Schiller's review [34] and references therein, it has been shown that certain conformations of enkephalin play an important role for the function. It is therefore interesting to see whether the Becke 3LYP/6-31G* level can correctly reproduce the geometries of the conformations and the interactions which stabilize these conformations.

From table 1 we can see that in many cases the SCC-DFTB and SCC-DFTB-D levels of theory appear to have different topologies, that is, the potential energy surfaces (PESs) not only have different numbers of local minima, but even different locations of the similar equivalent minima. The difference between the two levels, the addition of the empirical dispersion term, seems to not only add or correct for a small term in the energy, but also changes the topology. Hence it is very important to document this work further [55]. What we want to emphasize here is that, from the 30 original structures starting from the crystal

structures and the model structures, we ended up with 45 structures. This resulted from our using the SCC-DFTB and SCC-DFTB-D levels of theory as an intermediate level for our Becke 3LYP level structural optimization. Similarly, one can use one of many semi-empirical methods, for example, AM1 [86], PM3 [87], OM1 and OM2 [88, 89], or one of the many MM force fields. But our work here shows that one must be very careful with these preliminary pre-optimization steps, due to the differences in the topology of the PES for the different levels of theory. Since a lot of extra computational time would have to be used if one started from the crystal or NMR structures (if there are many structures or possible ways to add the hydrogens for a few structures), then we propose that one freezes the torsion angles at the values found in the experimentally determined structure. One has then ensured at the highest level one wishes to model that the system is the same local minimum. But we think it also important, at this early and developmental phase of MM, semi-empirical and approximate DFT theories and/or parametrizations, that the results starting from the intermediate level of theory optimized structures also be presented. This will allow us all to critically evaluate these new methods. Recently a heated discussion has occurred in the literature with respect to such an issue for the use of and development of van Der Waals parameters in some simulation studies [90, 91]. Hence it is very important to fully document not only one's level of theory, but also how the parameters were derived, and to publish them with the original paper or minimally deposited in the journal's archive where they can be readily downloaded, similar to what has been implemented for the deposition of crystal and NMR structures. Since the SCC-DFTB-D level also involves using the dispersion energy term based on parametrization, it must be critically evaluated. We are further investigating this relatively newly developed approximate DFT level of theory. Since it is an approximate DFT level, and DFT with a given XC is itself an approximate theory to full DFT, it is very important that any further corrections be correctly added and possibly be added already at the level of the parametrization. But this is impeded by a lack of highly accurate dispersion data for various configurations of the nuclei in the molecules and molecular systems. This is very similar to the problems encountered in parametrizing a given MM functional form in the classical force field parameterizations [45].

For the Becke 3LYP/6-31G* geometry optimizations with Gaussian98, we have used the new optimizer which uses a combination of internal and Cartesian coordinates. Irrespective of the input, either in Z-matrix or Cartesian coordinates, the gradients of the energy are minimized. There is a cut-off for the maximum force, maximum displacement, maximum RMS force and maximum RMS displacement. In many cases this optimizer fails to satisfy all of these criteria, especially the maximum displacement, for large flexible molecules like LeuE. This is due to the very shallow and flat potential energy surface along the torsional coordinates. In many cases the energy does not change and the optimization is either stopped by the program or manually.

3.2. Vibrational spectra

In addition to having predictions for the low energy conformers expected to be populated at room temperature, it is important to supplement this theoretical investigation with more experimental results. Since we have previously shown that the combination of vibrational absorption (VA), vibrational circular dichroism (VCD), Raman scattering and Raman optical activity (ROA) can answer such questions, both in non-polar solvents [8] and in aqueous solution [3, 6, 7], spectral simulations of the vibrational spectra for LeuE should motivate experimentalists to measure the VA, VCD, Raman and ROA spectra of LeuE.

In figures 3, 5, 7, 9 and 11 we present the s10ndp, s4ndp, s7ndp, d2ndp and d1ndp structures from table 1, and in figures 4, 6, 8, 10 and 12 the corresponding VA, VCD and Raman spectral

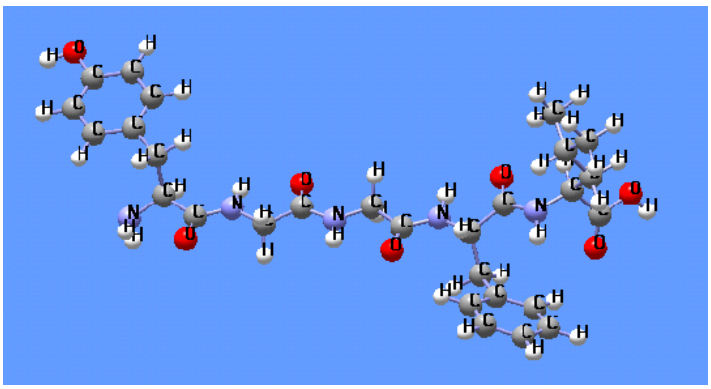

Figure 1. LeuE linear structure.

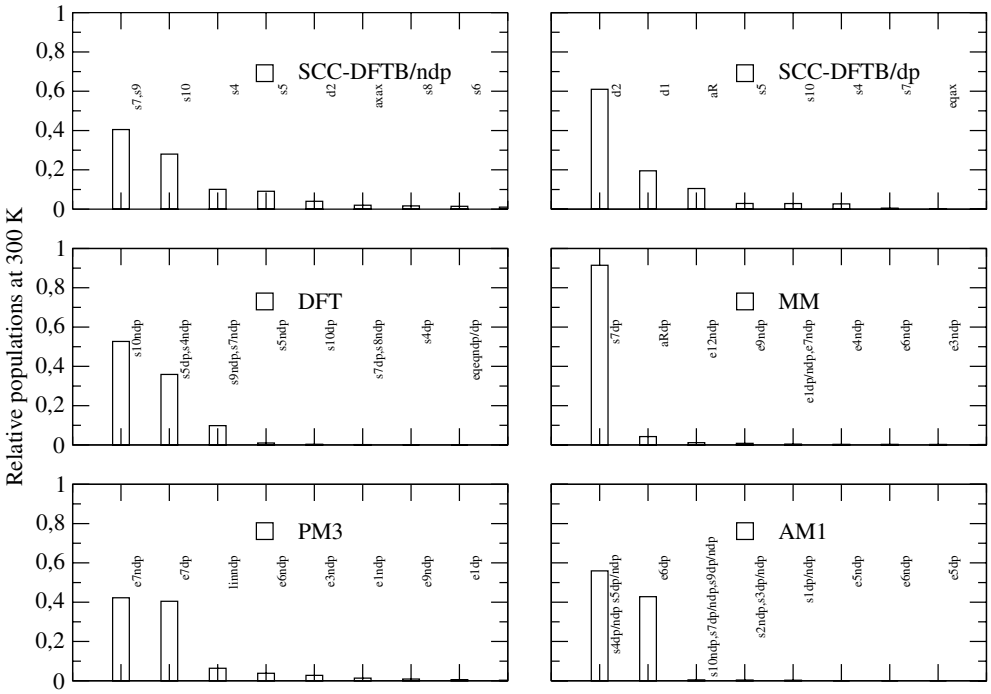

Figure 2. Probability distribution of conformers of LeuE as calculated using Boltzmann statistics using only the relative energies of the conformers in kcal mol^{-1}. Becke 3LYP/6-31G* energies are from table 1, SCC-DFTB, AM1, PM3 and MM results from [55].

simulations. The VA and VCD spectral simulations for the low energy conformers of LeuE have recently been compared to the measured spectra in DMSO-d_6 and been used to assign the conformers present. As one can see in figure 4 the mid-infrared (IR) region is very rich in features and large intensities relative to the other regions in the VA and VCD spectra, while in the Raman the intensities above 2900 cm^{-1} are much larger relative to the mid-IR and other regions. Hence the measurements are complementary. The normal modes are of course the same, so the frequency information is the same, but since the intensities are based on different

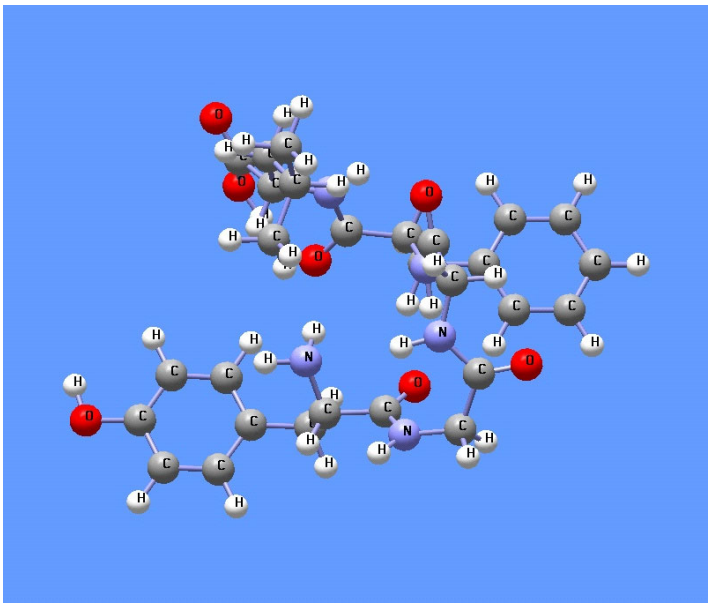

Figure 3. LeuE s10ndp structure.

selection rules, we gain different information from the VA, VCD and Raman intensities. The VA intensities are proportional to the change in the electric dipole moment during the normal mode. Hence modes which have large IR intensities are those which involve motions of the polar groups. The group modes for the amide groups, the N-terminus and the C-terminus are very intense in the IR; the deformation modes are mainly in the region between 1000 and 2000 cm^{-1} and the stretch modes of the N–H and O–H group hydrogens above 3300 cm^{-1}. Between 2900 and 3200 cm^{-1} we see the CH group hydrogen stretch modes, weak in the IR but very intense in the Raman. These characteristic modes have been used to identify which functional groups are actually present in the molecule and in many cases the ionization state of the functional groups which have more than one ionization state. For example, the N-terminus can be in either the neutral NH_2 form or the cationic positively charged NH_3^+ from. Similarly, the C-terminus can be in the neutral COOH form or the anionic negatively charged COO^- form. Similarly the OH group of the Tyr group can be in the neutral OH form or the anionic negatively charged O^- form. The IR modes for these groups are different and can be used to definitively assign the ionization state of these groups. In addition to the ionization state of certain groups, the VA, VCD and Raman spectra can in many cases be used to identify which conformer or conformers are present. That is what has really motivated our work here, that is, to simulate the VA, VCD and Raman spectra for the low energy conformers so as to be able to determine which conformer or conformers are actually present, with the assumption that our simulations are accurate enough to do so.

In figure 13 we present the new chemically modified LeuE we found by the proton transfer from the N-terminus ammonium group to the oxygen of the amide group of Phe residue with the concerted bond formation to form the five-membered ring. In figure 14 we also present the simulated VA, VCD and Raman spectra for this species. Finally, in figure 15 we present our predicted zwitterionic form of LeuE starting from the single-β-bend crystal structure. Here we have a stable species. The backbond angles ψ_1, (ϕ_2 and ψ_2), (ϕ_3 and ψ_3), (ϕ_4 and ψ_4) and

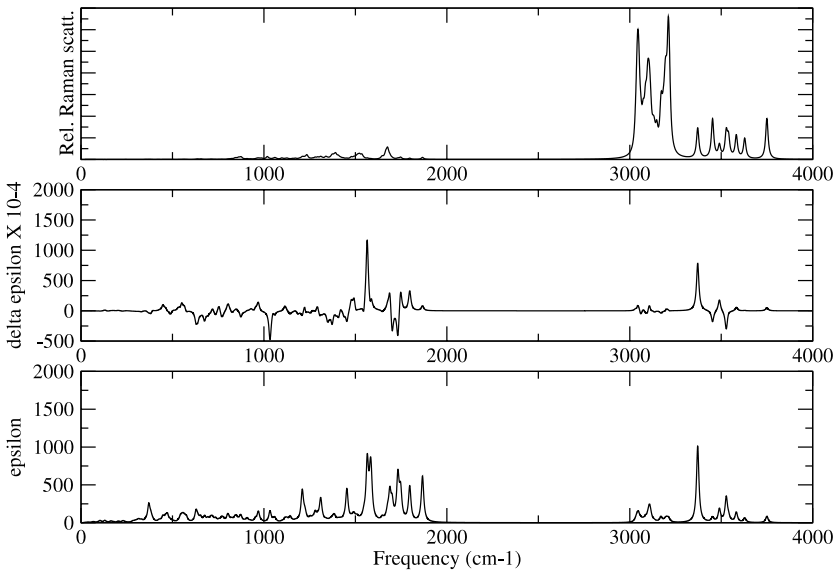

Figure 4. VA, VCD and Raman spectra of the s10ndp structure. Hessian, atomic polar, atomic axial tensors and EDEDPD were all calculated at the Becke 3LYP/6-31G* level of theory.

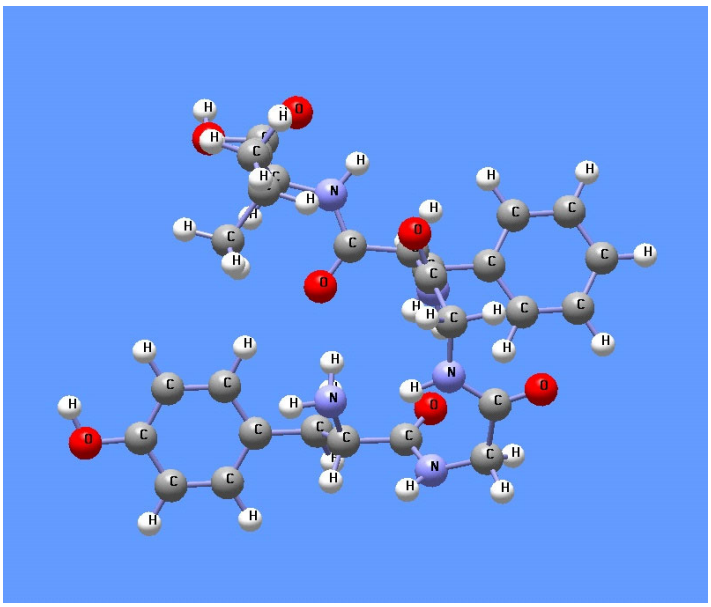

Figure 5. LeuE s4ndp structure.

ϕ_5 have the values $-168°$, $72°$, $26°$, $63°$, $26°$, $-120°$, $145°$ and $-152°$, respectively. We have also optimized the structure of neutral non-ionic species of LeuE at the Becke 3LYP + Onsager level. The backbond angles ψ_1, (ϕ_2 and ψ_2), (ϕ_3 and ψ_3), (ϕ_4 and ψ_4) and ϕ_5 have the values $93°$, $64°$, $13°$, $-132°$, $-19°$, $-77°$, $89°$ and $-120°$, respectively. Hence one can see that by the simple proton transfer one can induce a conformational change which is propagated along the

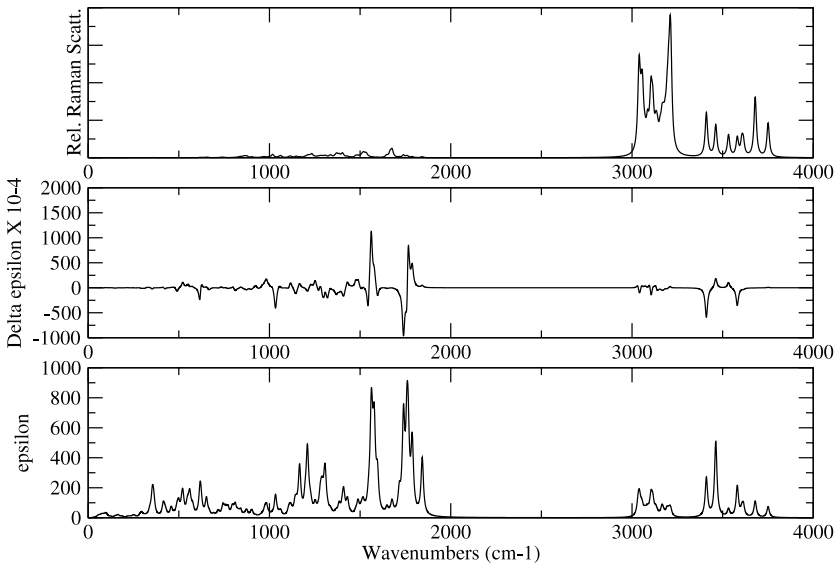

Figure 6. VA, VCD and Raman spectra of the s4ndp structure. Hessian, atomic polar, atomic axial tensors and EDEDPD were all calculated at the Becke 3LYP/6-31G* level of theory.

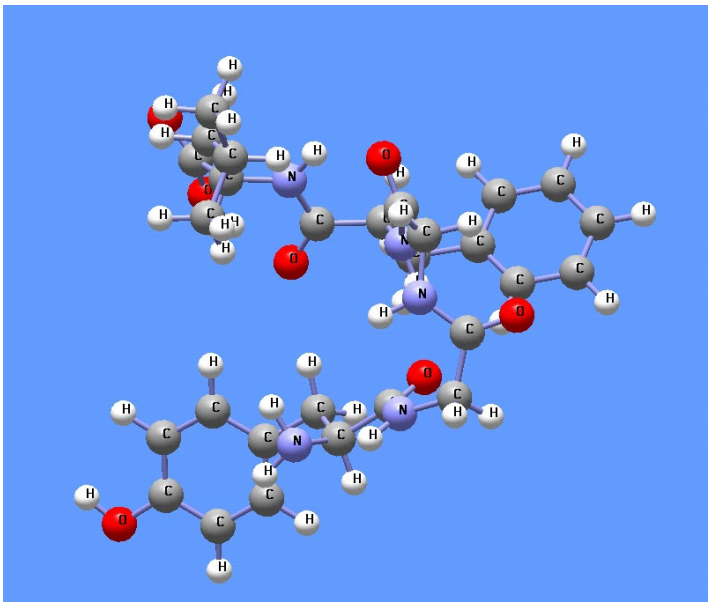

Figure 7. LeuE s7ndp structure.

backbone from one end of the peptide (or protein?) to the other end. It will also be interesting to see whether this effect is also seen in QM/MD studies. We hope to present the results of those simulations in the near future.

The simulated VA, VCD and Raman spectra for the s10ndp, s4ndp and s7ndp structures, the three structures which are predicted to be significantly populated at room temperature

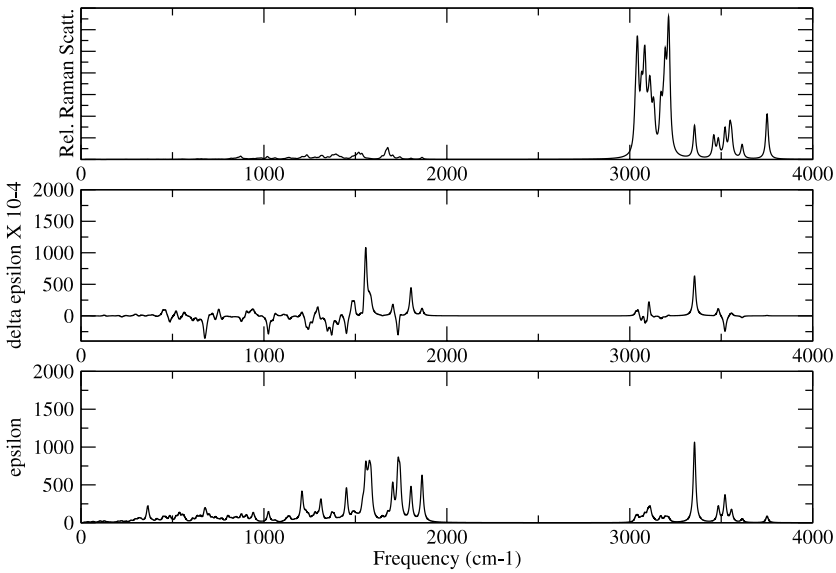

Figure 8. VA, VCD and Raman spectra of the s7ndp structure. Hessian, atomic polar, atomic axial tensors and EDEDPD were all calculated at the Becke 3LYP/6-31G* level of theory.

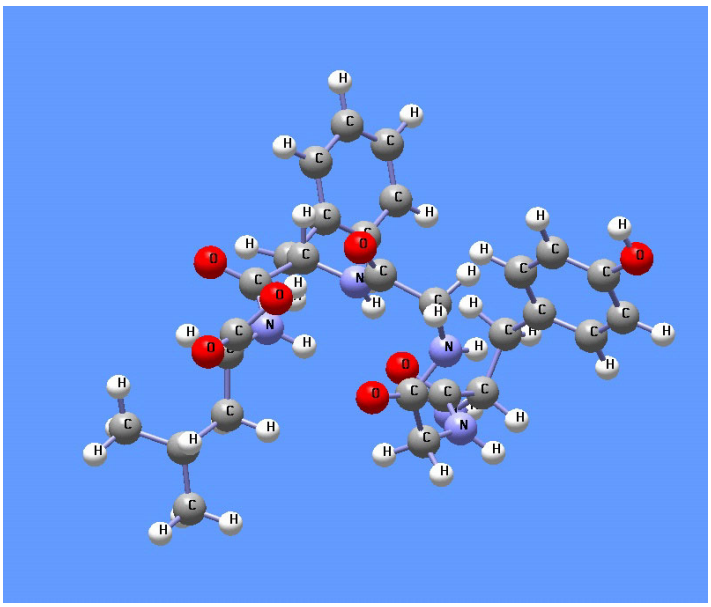

Figure 9. LeuE d2ndp structure.

for LeuE in a non-polar non-hydrogen-bonding solvent or in an Ar or N_2 low temperature matrix, can be compared to each other. It is clearly seen visually from the spectral simulations that the combination of VA, VCD and Raman spectra is much better in identifying which conformer or conformers are present than the use of only the VA and Raman spectra. With the recent availability of commercial VCD instrumentation, the use of this new technique,

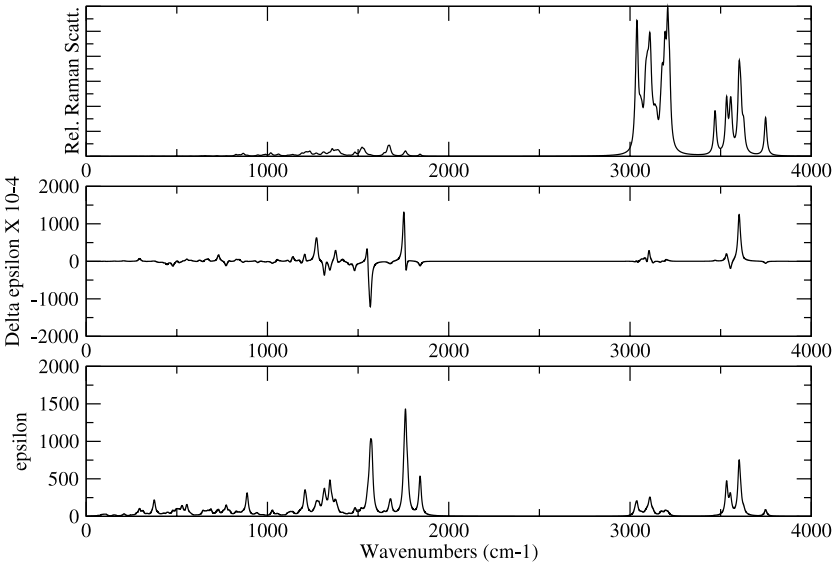

Figure 10. VA, VCD and Raman spectra of the d2ndp structure. Hessian, atomic polar, atomic axial tensors and EDEDPD were all calculated at the Becke 3LYP/6-31G* level of theory.

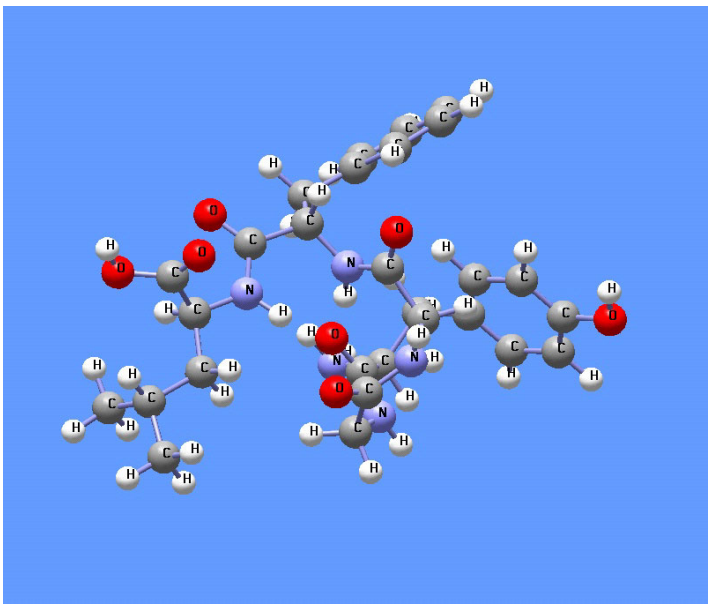

Figure 11. LeuE d1ndp structure.

in combination with the VA and Raman spectra, holds a promising future for structural and functional studies of peptides and proteins, where x-ray and NMR studies have not been able to provide this information. Hence this combination should be seen as complementary to the conventional x-ray and NMR techniques in structural and functional studies of biomolecules. Previously VA and VCD spectral measurements and spectral simulations of the VA and VCD

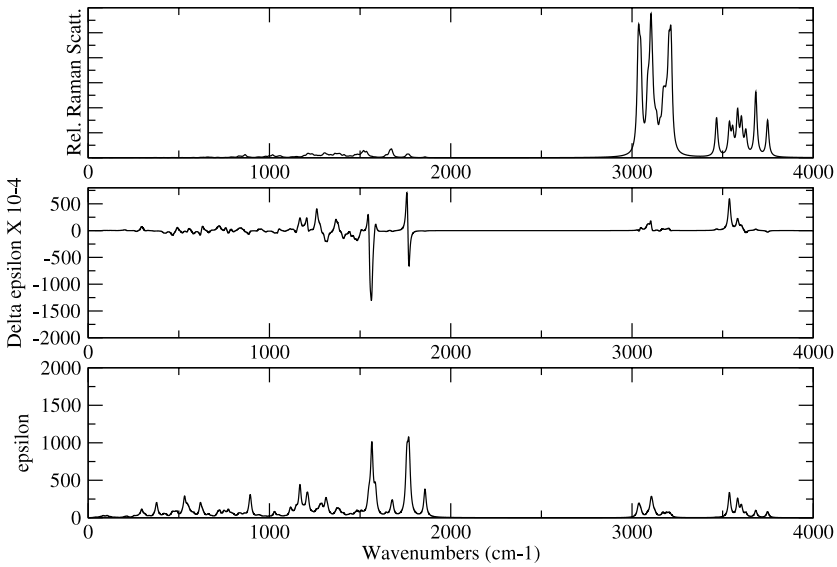

Figure 12. VA, VCD and Raman spectra of the d1ndp structure. Hessian, atomic polar, atomic axial tensors and EDEDPD were all calculated at the Becke 3LYP/6-31G* level of theory.

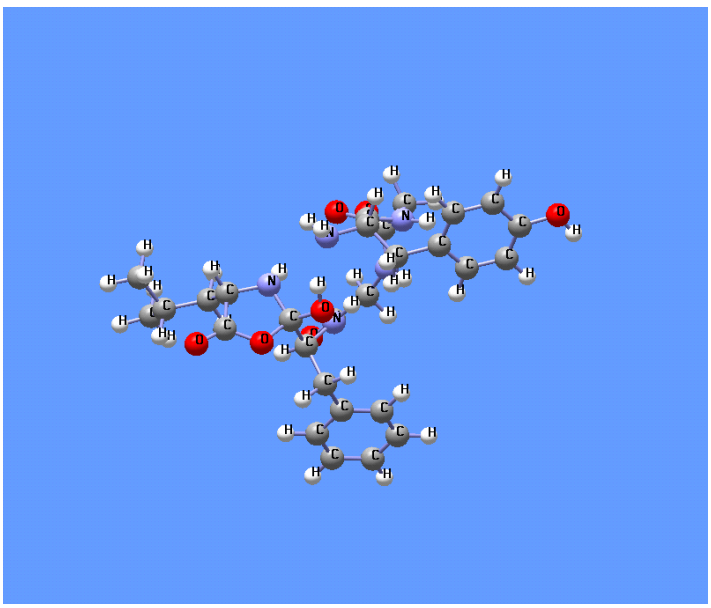

Figure 13. Chemically modified Leu-enkephalin structure (new structure, starting from the d2 zwitterionic structure).

spectra, with the additional Raman and ROA measurements and simulations, have been able to identify the conformers of LA and NALANMA in aqueous solution [6, 7] and NALANMA in non-polar solvents [8]. It is hoped that in the near future VA, VCD, Raman and ROA spectral measurements will be able to answer the same question for LeuE, now that the spectral simulations have been presented in this work for the VA, VCD and Raman spectra.

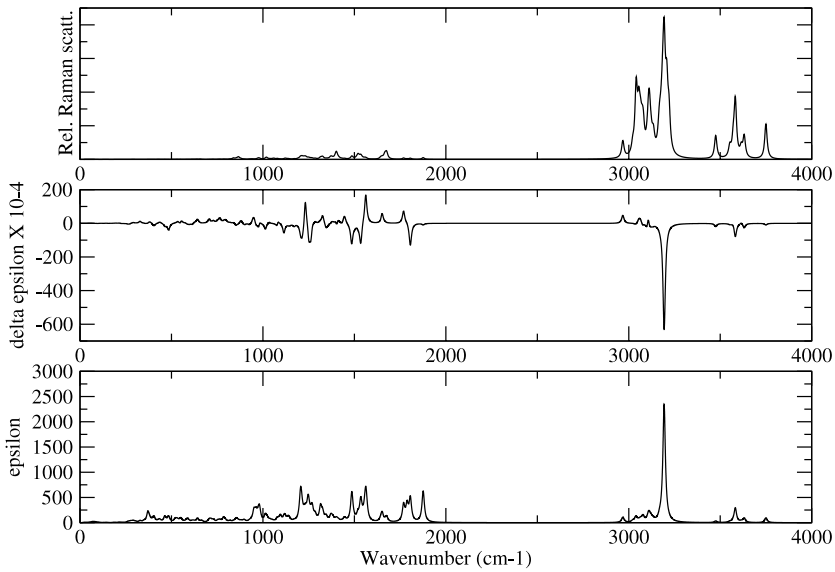

Figure 14. VA, VCD and Raman spectra of the new structure (starting from d2 zwitterionic structure) Hessian, atomic polar, atomic axial tensors and EDEDPD were all calculated at the Becke 3LYP/6-31G* level of theory.

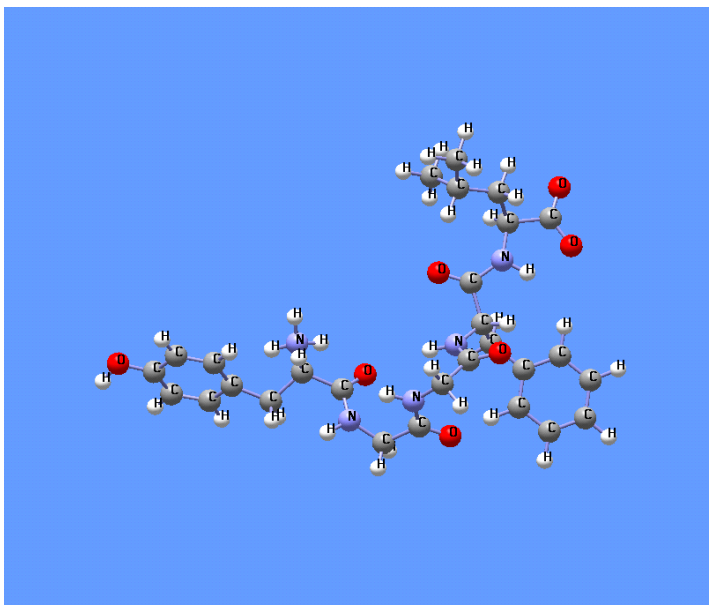

Figure 15. Neutral zwitterionic form of LeuE at Becke 3LYP + Onsager level of theory.

In addition, in figures 9 and 11 are presented the simulated VA, VCD and Raman spectra for the d2 and d1 conformers of LeuE. Even though these conformers are higher in energy in our calculations, by presenting these spectra, these conformers may be identified in spectra made under different solvent conditions; hence it is important to also present the spectra for the

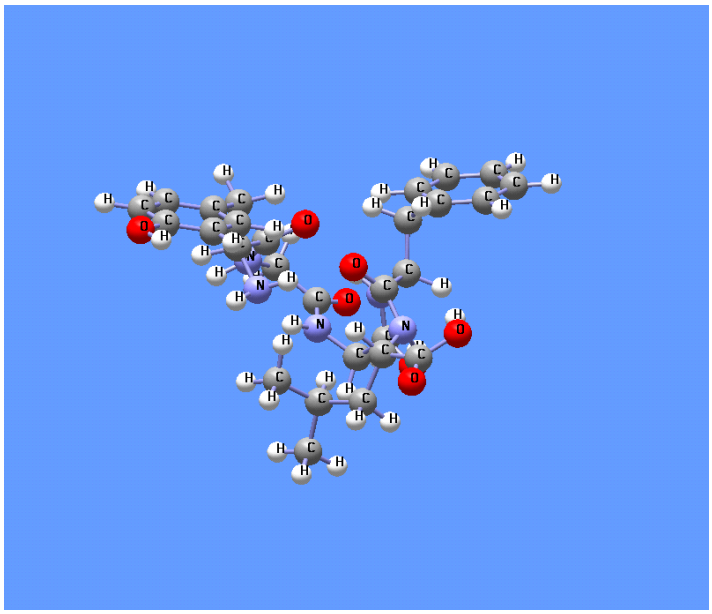

Figure 16. Neutral non-ionic form of LeuE at Becke 3LYP + Onsager level of theory.

higher energy conformers. These two conformers are also predicted to be populated at room temperature at the SCC-DFTB-D level of theory [55] as shown in figure 2. The simulated spectra for the complete set of conformers given in table 1 will be presented in a future work.

Even though our calculations presented here for LeuE without the Onsager treatment are strictly speaking for LeuE in the isolated state, we have recently compared them to the measured VA spectra of dimethylsulfoxide (DMSO)-d_6 [92]. Here we were able to propose which structure was present in this solvent, but we were required to make additional VCD measurements and have recently presented our comparison with these new experimental results [93]. But since DMSO can hydrogen bond via the oxygen of the sulfoxide group with the hydrogens of either the nitrogen of the N-terminus or the hydrogens of the amide groups of the backbone, which we have not taken into account here, this use of our calculations is not optimal. But the results, even though not optimal, have been used and the structure has been proposed based on the comparison. The Raman simulations presented here can also be used to further check whether the structure proposed from the VA and VCD spectra is indeed consistent with the Raman measurements. Hence it is important to simulate the spectra for all three forms of the vibrational spectroscopic measurement. Additionally, it would be nice to also have the predicted ROA spectra for the various conformers of LeuE. To date there have been no reported ROA spectra for LeuE, but such investigations are now underway in the laboratory of Professor Hug in Zurich. These additional experiments and our subsequent simulations will hopefully definitely answer the question of which conformers of LeuE are populated at room temperature. Also, the Raman spectra of LeuE as a function of pH has recently been reported, but with no theoretical analysis of the spectra. Since these spectra were also in aqueous solution, we do not compare to them, but leave that for a future publication. In addition, it has recently been reported that the zwitterionic form of LeuE is also present in DMSO solution. Hence the analysis of the DMSO VA and VCD spectra of LeuE recently reported should be reanalysed to take this into account.

4. Summary and conclusions

We have performed geometry optimizations starting from the reported crystal structures and six other commonly found structures of LeuE. Since the crystal structures did not report the hydrogens, this was the first step which needed to be performed. After determining where the hydrogens should be placed, SCC-DFTB and SCC-DFTB-D level geometry optimizations were performed, which have then been used as starting points for Becke 3LYP/6-31G* level geometry optimizations [55]. For the predicted low energy conformers which are expected to be populated at room temperature, we have additionally simulated the VA, VCD and Raman spectra. By measuring the VA, VCD and Raman spectra of LeuE in non-polar solvents, these predicted spectra can be compared to experimental spectra to identify which, if indeed any, of our predicted structures are populated. Our simulated VA and VCD spectra have recently been compared to the measured VA and VCD spectra of LeuE in DMSO-d_6. Here, based on the agreement between the measured and theoretical simulations, the structure present in DMSO has been proposed. Here only the non-ionic neutral species of LeuE was taken into account.

In addition, we recommend that the conformational energy surface of LeuE and other larger polypeptides should be used as new benchmarks for testing new and current semi-empirical and MM methods and/or parametrizations, rather than the potential energy surface for the alanine dipeptide and other small peptides, as has been previously used. This work gives a large set of conformational energies which can be used as a test set. In a future work we will expand upon this and also include a potential energy surface for the zwitterionic species of LeuE in aqueous solution, similar to the one we have presented for the alanine dipeptide [6]. Here we have only presented our preliminary zwitterionc structure determined at the Becke 3LYP + Onsager level of theory. Our attempts to determine the structure of the neutral zwitterionic form of LeuE using the COSMO model as implemented in Gaussian98 all failed. There have also been previously reported problems of convergence with the COSMO and other continuum models for strongly hydrogen bonding systems. These continuum models are better suited for non-polar molecules.

Here we have only treated the effects due to the bulk water, and our previous works have shown that for molecules like LeuE it is important to treat the first solvent shell layers of waters explicitly and then treat the effects due to bulk water by either a MM model, the so called QM/MM, or a continuum model. In the case of applying the QM/MM model to LeuE and other peptides, we also advocate a hybrid model, that is, to treat the first solvent shell layer of water molecules in addition to the solute quantum mechanically, and then only the second and third solvation shells and further with the MM model.

In addition to the VA, VCD spectra, and Raman scattering, the ROA spectra would also be of interest. But here one would require the calculation of, in addition to the EDEDPD, the electric dipole–electric quadrupole polarizability derivative (EDEQPD) and the electric dipole–magnetic dipole polarizability derivative (EDMDPD) tensors. The EDEDPD and EDEQPD are not too difficult to implement, as they are similar to the electric dipole moment, and can be calculated by finite field perturbation theory. The calculation of the EDMDPD would require the addition of a magnetic field, similar to the early work of Lowe and Stephens [94]. Other alternatives are extensions of the coupled perturbed Hartree–Fock implementation of Amos *et al* [74] and of the sum over excited states implementation via the random phase approximation of Lazzeretti and Zanasi [95]. In addition to the VA, VCD, Raman and ROA spectra one can also gain configurational and conformational information about amino acids and peptides via specific rotation measurements [96]. Here one requires the structure of the molecule and then one needs to calculate electric dipole–magnetic dipole polarizability EDMDP [97, 98].

These are the tensors of which we need the nuclear derivatives to calculate the ROA spectral intensities.

The calculation of the nuclear magnetic resonance shielding tensors has already been implemented in an extension to the SCC-DFTB method, so there is hope that in the near future the SCC-DFTB and other semi-empirical methods will be able to be used to predict the VA, VCD, Raman and ROA spectra of biomolecules. The scalability of the method makes these methods very important for biomolecular modelling. Also, to ultimately treat the protein environment will require one to probably treat a large part of the protein with a classical force field and the active site and/or region of interest with either a high level *ab initio* method (MP2, MCSCF, coupled cluster etc), a hybrid or GGA DFT method (Becke 3LYP) or a semi-empirical method (SCC-DFTB, AM1, PM3, OM1, OM2 etc) [89], the so-called QM/MM/MD methodology. Here there are a variety of ways to treat the frontier between the active site (QM region) and the classical force field region (MM) [99–107].

To simulate the VA, VCD, Raman and ROA tensors at present requires that these tensors be calculated at either the SCF or DFT levels of theory and combined with either *ab initio*, MM or semi-empirical Hessians. Early work though has shown that the most sensitive part of the VA, VCD, Raman and ROA intensities is to have an accurate geometry and Hessian. Here one really requires that one has an accurate description of the vibrational modes. Hence an accurate reproduction of the VA, VCD, Raman and ROA intensities is a very good test of either an *ab initio*, semi-empirical or empirical method to reproduce the dynamical motions of a biomolecule. In the future, one could even foresee the use of these experimental data in both non-polar solvents and aqueous solution in the parametrization schemes. Many of the more recent semi-empirical and approximate DFT methods have attempted to take in electron correlation terms and/or dispersion effects, which are hard and expensive to calculate even for the fully *ab initio* methods. Hence there is a lack of good experimental and theoretical data to not only use in the parametrization, but also to test the parametrization afterwards. The VA, surface-enhanced VA (SEVA) VCD, Raman, SERS and ROA intensities have a lot of information, especially if one can measure the polarization properties of these by making measurements on single oriented molecules. With the advent of the SEVA and SERS spectroscopy, this is probably possible in the not so distant future. The real challenge will also be to make SEVCD and SEOROA measurements on individual oriented molecules. This remains to be seen, but is an interesting challenge on the experimental side, as its prediction is on the theoretical side.

In an additional future work we will give a complete description of all of the structures found to date as well as performing molecular dynamics simulations for LeuE in non-polar solvents. This is necessary to find the global minimum of such a large molecule as LeuE. Other possibilities would be to perform a simulated annealing simulation, genetic algorithm search or Monte Carlo search. There have been many such simulations to date with various empirical and semi-empirical methods, but to date there is no consensus as to the structure of LeuE in its various environments, be it aqueous solution at various pHs and ionic strengths, in non-polar solvents or embedded in the membrane. Our work here has not answered the question definitively either, but we have provided some benchmark calculations against which the empirical and semi-empirical methods can be tested, before using them to do a large scale simulation in search for the global minimum. We have also presented the VA, VCD and Raman spectra for five low energy conformers of LeuE which already have motivated the spectral measurements and identification of the conformers present of LeuE in DMSO-d_6. It would also be nice to see the VA, VCD and Raman spectra of LeuE isolated in low temperature Ar or N_2 matrix or in the gas phase, which are the experiments which would be the closest to our simulations. In addition we have presented the zwitterionic form of LeuE at the Becke 3LYP/6-31G* + Onsager level of theory. In the near future we hope to extend this work to

the other conformers and also include explicit waters and then explicit waters plus either a continuum solvent treatment of the bulk waters or an MM level treatment.

Acknowledgments

The author would like to acknowledge the Danish National Research Foundation for the funding of the Quantum Protein (QuP) Centre in the Department of Physics at the Technical University of Denmark, 2800 Lyngby, Denmark. He would also like to acknowledge Carme Roviva at the Centre de Quimica Teorica, Parc Cientific de Barcelona, 08028 Barcelona, Spain, for financial support for a stay in Barcelona. Computational support through the Department of d'Arquitecura de Computadors, Modul C6-208, Campus Nord, UPC, 08034 Barcelona, is also gratefully acknowledged.

References

[1] Jalkanen K J, Nieminen R M, Knapp-Mohammady M and Suhai S 2003 Vibrational analysis of various isotopomers of L-alanyl-L-alanine in aqueous solution: vibrational absorption (VA), vibrational circular dichroism (vcd), Raman and Raman optical activity (ROA) spectra *Int. J. Quantum Chem.* **92** 239–59

[2] Abdali S, Jalkanen K J, Bohr H, Suhai S and Nieminen R M 2002 The VA and VCD spectra of various isotopomers of L-alanine in aqueous solution *Chem. Phys.* **282** 219–35

[3] Jalkanen K J, Nieminen R M, Frimand K, Bohr J, Bohr H, Wade R C, Tajkhorshid E and Suhai S 2001 A comparison of aqueous solvent models used in the calculation of the Raman and ROA spectra of L-alanine *Chem. Phys.* **265** 125–51

[4] Frimand K, Jalkanen K J, Bohr H G and Suhai S 2000 Vibrational absorption and vibrational circular dichroism analysis of L-alanine in aqueous solution: a density functional and RHF study *Chem. Phys.* **255** 165–94

[5] Knapp-Mohammady M, Jalkanen K J, Nardi F, Wade R C and Suhai S 1999 L-alanyl-L-alanine in the zwitterionic state: structures determined in the presence of explicit water molecules and with continuum models using density functional theory *Chem. Phys.* **240** 63–77

[6] Han W-G, Jalkanen K J, Elstner M and Suhai S 1998 Theoretical study of aqueous N-acetyl-L-alanine N′-methylamide: structures and Raman, VCD and ROA spectra *J. Phys. Chem.* B **102** 2587–602

[7] Tajkhorshid E, Jalkanen K J and Suhai S 1998 Structure and vibrational spectra of the zwitterion L-alanine in the presence of explicit water molecules: a density functional analysis *J. Phys. Chem.* B **102** 5899–913

[8] Jalkanen K J and Suhai S 1996 N-acetyl-L-alanine N′-methylamide: a density functional analysis of the vibrational absorption and vibrational circular spectra *Chem. Phys.* **208** 81–116

[9] Head-Gordon T, Head-Gordon M, Frisch M J, Brooks C L and Pople J A 1991 Theoretical study of blocked glycine and alanine peptide analogs *J. Am. Chem. Soc.* **113** 5989–97

[10] Arkin H, Yasar F, Celik T, Berg B A and Meirovitch H 2002 Multicanonical simulation of some peptides *Comput. Phys. Commun.* **147** 600–3

[11] Yasar F, Arkin H, Celik T, Berg B A and Meirotitch H 2002 Efficiency of the multicanonical simulation method as applied to peptides of increasing size: the heptapeptide deltorphin *J. Comput. Chem.* **23** 1127–34

[12] Garduno-Juarez R, Morales L B and Flores-Perez P 2001 About singularities at the global minimum of empiric force fields for peptides *J. Mol. Struct. (Theochem)* **543** 277–84

[13] Kriz Z, Carlsen P H J and Koca J 2001 Conformational features of linear and cyclic enkephalins. A computational study *J. Mol. Struct. (Theochem)* **540** 231–50

[14] Yasar F, Celik T, Berg B A and Meirotitch H 2000 Multicanonical procedure for continuum peptide models *J. Comput. Chem.* **21** 1251–61

[15] Klepeis J L and Foudas C A 1999 Free energy calculations for peptides via deterministic global optimization *J. Chem. Phys.* **110** 7491–512

[16] van der Spoel D and Berendsen H J C 1997 Molecular dynamics simulations of Leu-enkephalin in water and DMSO *Biophys. J.* **72** 2032–41

[17] Androulaiks L P, Maranas C D and Floudas C A 1997 Prediction of oligopeptide conformation via deterministic global optimization *J. Global Opt.* **11** 1–34

[18] Baysal C and Meirovitch H 1997 Efficiency of the local torsional deformations method for identifying the stable structures of cyclic molecules *J. Phys. Chem.* A **101** 2185–91

[19] Meirovitch H, Meirovitch E, Michel A G and Vasquez M 1994 A simple and effective procedure for conformational search of macromolecules: application to Met- and Leu-enkephalin *J. Phys. Chem.* **98** 6241–3

[20] Meirovitch H and Meirovitch E 1996 New theoretical methodology for elucidating the solution structure of peptides from NMR data. 3. Solvation effects *J. Phys. Chem.* **100** 5123–33
[21] Han W-G and Suhai S 1996 Density functional studies of N-methylacetamide–water complexes *J. Phys. Chem.* **100** 3942–9
[22] Aubry A, Birlirakis N, Sakarellos-Daitsiotis M, Sakarellos C and Marraud M 1989 A crystal molecular conformation of leucine-enkephalin related to the morphine molecule *Biopolymers* **28** 27–40
[23] Smith G D and Griffin J F 1978 Conformation of [leu^5]enkephalin from x-ray diffraction: features important for recognition at opiate receptor *Science* **199** 1214–16
[24] Griffin J F, Langs D A, Smith G D, Blundell T L, tickle I J and Bedarkar S 1986 The crystal structures of [met^5]enkephalin and a third form of [leu^5]enkephalin: observations of a novel pleated β-sheet *Proc. Natl Acad. Sci. USA* **83** 3272–6
[25] Karle I L, Karle J, Mastropaolo D, Camerman A and Camerman N 1983 [leu^5]enkephalin: four cocrystallizing conformers with extended backbones that form an antiparallel β-sheet *Acta Crystallogr.* B **39** 625–37
[26] Kimura A, Naohito K and Fujiwara 1996 Orientation and conformation of Met-enkephalin in a liquid crystal as studied by magic-angle- and near-magic-angle-spinning two-dimensional NMR spectroscopy *J. Phys. Chem.* **100** 14056–61
[27] Kimura A, Takamoto K and Fujiwara H 1998 Conformatinal diversity of [d-pen^2,d-pen^5]enkephalin as studied by magic angle spinning liquid-crystal NMR spectroscopy and multiconformational analysis *J. Am. Chem. Soc.* **120** 9656–61
[28] Kimura A, Kuni N and Fujiwara H 1997 Conformation and orientation of Met-enkephalin analogues in a lyotropic liquid-crystal studied by the magic angle spinning two-dimensional methodology in nuclear magnetic resonance: relationships between activities and membrane-associated structures *J. Am. Chem. Soc.* **119** 4719–25
[29] Doi M, Ishibe A, Shinozaki H, Urata H, Inoue M and Ishida T 1994 Conserved and novel structural characteristics of enantiomorphic Leu-enkephalin *Int. J. Peptide Protein Res.* **43** 325–31
[30] Okuyama K and Ohuchi S 1996 Recent structural studies of peptides in Japan *Biopolymers (Peptide Science)* **40** 85–103
[31] Deschamps J R, George C and Flippen-Anderson J L 1996 Structural studies of opioid peptides: a review of recent progress in x-ray diffraction studies *Biopolymers (Peptide Science)* **40** 121–39
[32] Kosterlitz F R S and H W 1985 Opioid peptides and their receptors *Proc. R. Soc.* B **225** 27–40
[33] Wiest R, Pichon-Pesme V, Benard M and Lecomte C 1994 Electron distribution in peptides and related molecules experimental and theoretical study of Leu-enkephalin trihydrate *J. Phys. Chem.* **98** 1351–62
[34] Schiller P W 1948 *Peptides* **6** 219–68
[35] Berins J, Nikiforovich G V and Chipens G 1986 Statistical weights of Leu-enkephalin conformers in aqueous solution *J. Mol. Struct. (Theochem)* **137** 129–32
[36] Nishimura K, Naito A, Tuzi S, Saito H, Hashimoto C and Aida M 1998 Determination of the three-dimensional structure of crystalline Leu-enkephalin dihydrate based on six sets of accurately determined interatomic distances from ^{13}C-REDOR NMR and the conformation-dependent ^{13}C chemical shifts *J. Phys. Chem.* B **102** 7476–83
[37] Amodeo P, Naider F, Picone D, Tancredi T and Temussi P A 1998 Conformational sampling of bioactive conformers: a low-temperature NMR study of 15^N-Leu-enkephalin *J. Peptide Sci.* **4** 253–65
[38] Rudolph-Boehner S, Quarzago D, Czisch M, Ragnarsson U and Moroder L 1997 Conformational preferences of Leu-enkephalin in reverse micelles as membrane-mimicking environment *Biopolymers* **41** 591–606
[39] Gerothanassis I P, Karayannis T, Sakarellos-Daitsiotis M, Sakarellos C and Marraud M 1987 Nitrogen-14 nuclear magnetic resonance of the amino terminal group of Leu-enkephalin in aqueous solution *J. Magn. Reson.* **75** 513–16
[40] Behnam B A and Deber C M 1984 Evidence for a folded conformation of methionine-and leucine-enkephalin in a membrane environment *J. Biol. Chem.* **23** 1435–90
[41] Kimura A, Kano T and Fujiwara H Magnetic-angle-spinning two-dimensional NMR for the study of conformation of leucine-enkephalin oriented in a lyotropic liquid crystal
[42] Rommel-Möhle K and Hofmann H-J 1993 Conformational dynamics in peptides: quantum chemical calculations and molecular dynamics simulations on N-acetyl-L-alanyl-N$'$-methylamide *J. Mol. Struct. (Theochem)* **285** 211–19
[43] Brooks C L III and Case D A 1993 Simulations of peptide conformational dynamics and thermodynamics *Chem. Rev.* **93** 2487–502
[44] Cornell W D, Cieplak P, Bayly C I, Gould I R, Merz K M Jr, Fergusson D M, Spellmeyer D C, Fox T, Caldwell J W and Kollman P A 1995 A second generation force field for the simulation of proteins, nucleic acids and organic molecules *J. Am. Chem. Soc.* **117** 5179–97

[45] Maple J R, Hwang M-J, Jalkanen K J, Stockfisch T P and Hagler A T 1998 Derivation of class II force fields. V. A quantum force field for amides, peptides, and related compounds *J. Comput. Chem.* **19** 430–58
[46] Beglov D and Roux B 1995 Dominant solvation effects from the primary shell of hydration: approximation for molecular dynamics simulations *Biopolymers* **35** 171–8
[47] Elstner M 1998 Weiterentwichlung quantenmechanischer Rechenverfahren fuer organische Molekuele und Polymere *PhD Thesis* Universitaet-Gesamthochschule Paderborn
[48] Ordejon P, Artacho E and Soler J M 1996 Self-consistent order-*n* density-functional calculations for very large systems *Phys. Rev.* B **53** R10441
[49] Bohr H G, Jalkanen K J, Frimand K, Elstner M and Suhai S 1999 A comparative study of MP2, B3LYP, RHF and SCC-DFTB force fields in predicting the vibrational spectra of N-acetyl-L-alanyl-N′-methylamide: VA and VCD spectra *Chem. Phys.* **246** 13–36
[50] Elstner M, Jalkanen K J, Knapp-Mohammady M, Frauenheim Th and Suhai S DFT studies on helix formation in N-acetyl-(L-alanyl)$_n$-N′-methylamide for $n = 1$–20 *Chem. Phys.* **256** 2000
[51] Elstner M, Jalkanen K.J, Knapp-Mohammadi M, Frauenheim Th and Suhai S 2001 Energetics and structure of glycine and alanine based model peptides: approximate SCC-DFTB, AM1 and PM3 methods in comparison with DFT, HF and MP2 calculations *Chem. Phys.* **263** 203–19
[52] Elstner M, Hobza P, Suhai S and Kaxiras E 2001 Hydrogen bonding and stacking interactions of nucleic acids and base pairs: a density functional based treatment *J. Chem. Phys.* **114** 5149–55
[53] Frimand K and Jalkanen K J 2002 SCC-TB, DFT/B3LYP, MP2, AM1, PM3, and RHF study of ethylene oxide and propylene oxide structures, VA and VCD spectra *Chem. Phys.* **279** 161–78
[54] Lee C H and Zimmerman S S 1995 Calculations of the ϕ–ψ conformational contour maps for N-acetyl-L-alanine N′-methylamide and of the characteristic ratios of poly-L-alanine using various molecular mechanics force fields *J. Biomol. Struct. Dyn.* **13** 201–18
[55] Jalkanen K J, Jensen M, Bohr H G, Niehaus T, Elstner M, Suhai S and Frauenheim Th 2003 A study of the energetics and structures of [leu]-enkephalin based on SCC-DFTB, B3LYP, AM1, PM3 and Charmm force field methodologies *J. Phys. Chem.* A at press
[56] Khaled M A, Long M M, Thompson W D, Bradley R J, Brown G B and Urry D W 1977 *Biochem. Biophys. Res. Commun.* **76** 224
[57] Frisch M J and Forseman J B 1996 *Gaussian 98 User's Guide* (Pittsburg, PA: Gaussian) p 15106
[58] Becke A D 1993 Density-functional thermochemistry: the role of exact exchange *J. Chem. Phys.* **98** 5648
[59] Becke A D 1992 Density-functional thermochemistry. I. The effect of the exchange-only gradient correction *J. Chem. Phys.* **96** 2155
[60] Becke A D 1992 Density-functional thermochemistry. II. The effect of the Perdew–Wang generalized-gradient correlation correction *J. Chem. Phys.* **97** 9173
[61] Becke A D 1988 Correlation energy of an inhomogeneous electron gas: a coordinate-space model *J. Chem. Phys.* **88** 1053–62
[62] Lee C, Yang W and Parr R G 1988 Development of the Colle–Salvetti correlation-energy formula into a functional of the electron density *Phys. Rev.* B **37** 785
[63] Vosko S H, Wilk L and Nusair M 1980 Accurate spin-dependent electron liquid correlation energies for local spin density calculations: a critical analysis *Can. J. Phys.* **58** 1200–11
[64] Walters P and Stahl M B 2002 Version 1.6. Dolata Research Group, Department of Chemistry, University of Arizona, Tucson, Arizona 85721, USA
[65] Jalkanen K J, Bohr H G and Suhai S 1997 Density functional and neural network analysis: hydration effects and spectroscopic and structural correlations in small peptides and amino acids *Proc. Int. Symp. on Theoretical and Computational Genome Research (Spring Street, NY 1997)* ed S Suhai (New York: Plenum)
[66] Onsager L 1936 Electric moments of molecules in liquids *J. Am. Chem. Soc.* **58** 1486–93
[67] Person W and Zerbi G 1982 *Vibrational Intensities in Infrared and Raman Spectroscopy* (Amsterdam: Elsevier)
[68] Amos R D 1984 Dipole moment derivatives of H_2O and H_2S *Chem. Phys. Lett.* **108** 185–90
[69] Craig D P and Thirunamachandran T 1978 A theory of vibrational circular dichroism in terms of vibronic interactions *Mol. Phys.* **35** 825–40
[70] Stephens P J 1985 Theory of vibrational circular dichroism *J. Phys. Chem.* **89** 748–52
[71] Stephens P J 1987 Gauge dependence of vibrational magnetic dipole transition moments and rotational strengths *J. Phys. Chem.* **91** 1712–15
[72] Buckingham A D, Fowler P W and Galwas P A 1987 Velocity-dependent property surfaces and the theory of vibrational circular dichroism *Chem. Phys.* **112** 1–14
[73] Jalkanen K J, Stephens P J, Lazzeretti P and Zanasi R 1988 Nuclear shielding tensors, atomic polar and axial tensors, and vibrational dipole and rotational strengths of NHDT *J. Chem. Phys.* **90** 3204–13

[74] Amos R D, Handy N C, Jalkanen K J and Stephens P J 1987 Efficient calculation of vibrational magnetic dipole transition moments and rotational strengths *Chem. Phys. Lett.* **133** 21–6
[75] Amos R D, Jalkanen K J and Stephens P J 1988 Alternative formalism for the calculation of atomic polar tensors and atomic axial tensors *J. Phys. Chem.* **92** 5571–5
[76] Bak K L, Jørgensen P, Helgaker T, Ruud K and Jensen H J Aa 1993 Gauge-origin independent multiconfigurational self-consistent-field theory for vibrational circular dichroism *J. Chem. Phys.* **98** 8873–87
[77] Bak K L, Jørgensen P, Helgaker T, Ruud K and Jensen H J Aa 1994 Basis set convergence of atomic axial tensors obtained from self-consistent field calculations using London atomic orbitals *J. Chem. Phys.* **100** 6621–7
[78] Bak K L, Devlin F J, Ashvar C S, Taylor P R, Frisch M J and Stephens P J 1995 *Ab initio* calculation of vibrational circular dichroism spectra using gauge-invariant atomic orbitals *J. Phys. Chem.* **99** 14918–22
[79] Cheesman J R, Frisch M J, Devlin F J and Stephens P J 1996 *Ab initio* calculation of atomic axial tensors and vibrational rotational strengths using density fuctional theory *Chem. Phys. Lett.* **252** 211–20
[80] Cheeseman J R, Frisch M J, Devlin F J and Stephens P J 2000 Hartree–Fock and density functional theory *ab initio* calculation of optical rotation using GIAOs: basis set dependence *J. Phys. Chem.* A **104** 1039–46
[81] Amos R D 1986 Calculation of polarizability derivatives using analytic gradient methods *Chem. Phys. Lett.* **124** 376–81
[82] Frish M J, Yamaguchi Y, Gaw J F, Schaefer H F III and Binkley J S 1986 Analytic Raman intensities from molecular electronic wave functions *J. Chem. Phys.* **84** 531–3
[83] Johnson B G and Florian J 1995 The prediction of Raman spectra by density functional theory. Preliminary findings *Chem. Phys. Lett.* **247** 120–5
[84] Bunte S W, Jensen G M, McNesby K L, Goodin D B, Chabalowski C F, Nieminen R M, Suhai S and Jalkanen K J 2001 Theoretical determination of the vibrational absorption and Raman spectra of 3-methylindole and 3-methylindole radicals *Chem. Phys.* **265** 13–25
[85] Tajkhorshid E, Jalkanen K J and Suhai S 1998 Structure and vibrational spectra of the zwitterion L-alanine in the presence of explictit water molecules: a density functional analysis *J. Phys. Chem.* B **102** 5899–913
[86] Dewar J S, Zoebisch E, Healy E F and Stewart J J P 1985 *J. Am. Chem. Soc.* **107** 3902
[87] Stewart J J P 1989 *J. Comput. Chem.* **10** 209, 221
[88] Rommel-Möhle K, Hofmann H-J and Thiel W 2001 Description of peptide and protein secondary structures employing semiempirical methods *J. Comput. Chem.* **22** 509–20
[89] Thiel W 2000 *Modern Methods and Algorithms of Quantum Chemistry* vol 3 (Juelich: John Von Neuman Institute for Computing) ch Semiempirical Methods pp 261–83
[90] Aqvist J 1996 Comment to Daura, X. *Proteins* **25** 89–103
Aqvist J 1997 *Proteins: Structure Function Genetics* **28** 143
[91] Daura X, Oliva B, Querol E, Aviles F X and Tapia O 1996 On the sensitivity of MD trajectories to changes in water–protein interaction parameters. the potato carboxypeptidase inhibitor in water as a test case for the gromos force field *Proteins* **25** 89–103
[92] Abdali S, Niehaus T A, Jalkanen K J, Ciao X, Nafie L A, Frauenheim Th, Suhai S and Bohr H 2003 Vibrational absorption spectra, dft and scc-dftb conformational study and analyses of Leu-enkephalin *Phys. Chem. Chem. Phys.* **5** 1295–300
[93] Abdali S, Jalkanen K J, Ciao X, Nafie L A and Bohr H 2003 Conformational determination of Leu-enkephalin based on theoretical and experimental vibrational absorption and vibrational circular dichroism spectral analyses *Biophys. J.* submitted
[94] Stephens P J and Lowe M A 1985 Vibrational circular dichroism *Annu. Rev. Phys. Chem.* **36** 213
[95] Stephens P J, Jalkanen K J, Amos R D, Lazzeretti P and Zanasi R 1990 *Ab initio* calculations of atomic polar and axial tensors for HF, H_2O, NH_3, and CH_4 *J. Phys. Chem.* **94** 1811–30
[96] Ng K, Edkins T J and Bobbitt D R 1999 Direct specific rotation measurements of amino acids, dipeptides, and tripeptides by laser-based polarimetry *Chirality* **11** 187–94
[97] Stephens P J, Devlin F J, Cheeseman J R, Frisch M J, Mennucci B and Tomasi J 2000 Prediction of optical rotation using density functional theory: 6, 8-dioxabicyclo[3.2.1]octanes *Tetrahedron: Asymmetry* **11** 2443–8
[98] Stephens P J, Devlin F J, Cheeseman J R and Frisch M J 2001 Calculation of optical rotation using density functional theory *J. Phys. Chem.* A **105** 5356–71
[99] Gordon M S, Freitag M A, Bandyopadhyay P, Jensen J H, Kairys V and Stevens W J 2001 The effective fragment potential method: a qm-based mm approach to modeling environmental effects *J. Phys. Chem.* A **105** 293–307

[100] Reuter N, Dejaegere A, Maigret B and Karplus M 2000 Frontier bonds in QM/MM methods: comparison of different approaches *J. Phys. Chem.* A **104** 1720–35
[101] Murphy R B, Philip D M and Friesner R A 2000 A mixed quantum mechanics/molecular mechanics (qm/mm) method for large-scale modeling of chemistry in protein environments *J. Comput. Chem.* **21** 1442–57
[102] Day P N, Jensen J H, Gordon M S, Webb S P, Stevens W J, Krauss M, Garmer D, Basch H and Cohen D 1996 An effective fragment method for modeling solvent effects in quantum mechanical calculations *J. Chem. Phys.* **105** 1968–86
[103] Eurenius K P, Chatfield D C, Brooks B R and Hodoscek M 1996 Enzyme mechanisms with hybrid quantum and molecular mechanical potentials. I. Theoretical considerations *J. Comput. Chem.* **60** 1189–20
[104] Bakowies D and Thiel W 1996 Hybrid models for combined quantum mechanical and molecular mechanical approaches *J. Phys. Chem.* **100** 10580–94
[105] Gao J 1994 Computation of intermolecular interactions with a combined quantum mechanical and classical approach *Modeling the Hydrogen Bond (ACS Symp. Series 569)* (Washington, DC: American Chemical Society) pp 8–35
[106] Field M J, Bash P A and Karplus M 1990 A combined quantum mechanical and molecular mechanical potential for molecular dynamics simulations *J. Comput. Chem.* **6** 700–33
[107] Warshel A and Levitt M 1976 Theoretical studies of enzymic reactions *J. Mol. Biol.* **103** 227–49